This is an open access article published under an ACS AuthorChoice License, which permits copying and redistribution of the article or any adaptations for non-commercial purposes.

ACS OMEGA

http://pubs.acs.org/journal/acsodf

Article

Pickering Interfacial Catalysis—Knoevenagel Condensation in Magnesium Oxide-Stabilized Pickering Emulsion

Amid L. Sadgar, Tushar S. Deore, and Radha V. Jayaram*

Cite This: *ACS Omega* 2020, 5, 12224−12235

Read Online

ACCESS | Metrics & More | Article Recommendations | Supporting Information

ABSTRACT: In the present study, a novel catalytic route for the Knoevenagel condensation reaction has been developed by Pickering interfacial catalysis using magnesium oxide (MgO) as both an emulsion stabilizer and a base catalyst. MgO was prepared by the precipitation method using sodium hydroxide or ammonium hydroxide as the precipitating agent and calcined at different temperatures. The calcined samples were characterized by XRD, SEM, TEM, AFM, BET, and DLS techniques. The catalytic application of the emulsions stabilized by MgO was investigated for the Knoevenagel condensation reaction of benzaldehyde and its derivatives with malononitrile. All of the reactions were carried out at an ambient temperature (30 °C) under static conditions without stirring. Both the emulsion-stabilizing ability and the catalytic activity of MgO were found to be affected by the method of preparation, calcination temperature, and the nature of the oil phase. It was observed that the method of preparation varied the texture and morphology of MgO and thus the stability and droplet size of the emulsion formed. This was further reflected in the catalytic activity. The highest yield (87%) of the condensation product was obtained with MgO prepared by precipitation using a strong base (NaOH) and further calcined at 400 °C. The developed catalytic system offers several green chemistry advantages such as reusable solid-base catalyst and use of a single material as both emulsion stabilizer and catalyst. Room-temperature reaction under static conditions is an additional advantage of the developed catalytic system.

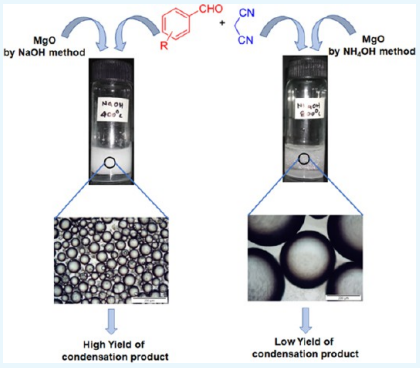

INTRODUCTION

Apart from the reacting chemicals, the choice of reaction medium is also important for the process to be qualified as benign. In the last few years, considerable attention has been directed toward identifying green alternatives to conventional volatile solvents in chemical transformations. Though water as a reaction medium is the most suitable choice, due to the hydrogen bonding present in water, many nonpolar compounds are hydrophobic and have very limited solubility.[1] To some extent, this problem of solubility can be overcome by the use of a suitable cosolvent. But this alternative introduces additional problems such as separation of solvents in large-scale applications. Carrying out the reaction in a pair of immiscible solvents (biphasic system) under vigorous mechanical agitation conditions is another alternative but not energetically favorable. Although phase-transfer catalysts[2] that transfer species across the interphase are applicable to many reaction systems, the problem associated with separation and reusability of catalysts still persists.[3] Reactions are also possible at the interface between a dispersed phase and a continuous phase. But the substantial increase in the interfacial area and hence the interfacial energy causes phase separation by several mechanisms. Emulsions are a stable biphasic system of two liquid phases that can be stabilized by suitable additives such as surfactants, enzymes, and polymers or some suitable solids.

Surfactant-stabilized emulsions and microemulsions systems have been well explored for various organic transformations like transfer hydrogenation,[4] photopolymerization,[5] oxidation,[6] hydroformylation,[7] and degradation of water pollutants.[8] Surfactant-stabilized emulsions can cause environmental issues as some surfactants are potentially toxic. Recovery of the system components is also a tedious process.[9] Hence, devising strategies to carry out a reaction in an emulsion stabilized by additives that are nontoxic and also easily recoverable will be a well sought-after green chemistry goal. Since most chemical reactions require a suitable catalyst to achieve considerable conversion and selectivity at ambient conditions, the choice of a reaction system that contains nontoxic additives, which not only make the reaction occur in a benign solvent like water but also function as a catalyst, would be of utmost importance to achieve green chemistry perspectives.

Percival Spencer Umfreville Pickering, a British chemist, reported as early as 1907 that emulsions can be stabilized by the adsorption of solid particles at an oil/water interface. In his honor, such emulsions are known as Pickering emulsions.[10] Pickering emulsions have wide applications in food[11] and

Received: February 24, 2020
Accepted: May 7, 2020
Published: May 19, 2020

ACS Publications

© 2020 American Chemical Society

pharmaceutical industries[12] and also in catalytic processes.[13] Pickering interfacial catalysis (PIC) is an emerging area of research in which a solid material acts both as a stabilizing agent and a catalyst at the interface. In PIC, enhanced interfacial area increases mass transfer and hence conversion and rate. Effective separation of final products, easy recovery of the catalyst, and the possibility to carry out reactions under static conditions are additional advantages of PIC.[14−18] Various types of organic transformation like oxidation,[19,20] hydrogenation,[21] hydroformylation,[22] deacetalization,[23] epoxidation,[24] hydrodeoxygenation,[25] hydrolysis,[26] and transesterification[27−29] have been reported through PIC.

Metal oxides have been extensively studied as catalysts as they can exhibit acidic, basic, and redox properties. A Pickering emulsion formed with a suitable metal oxide can be an excellent reaction medium and also a reusable catalytic system. Among the well-explored metal oxides, magnesium oxide (MgO) exhibits good catalytic activity and can be prepared with high surface area and porosity by suitably modifying the conditions of preparation.[30] Though it has been reported that magnesium oxide forms a stable Pickering emulsion,[31−33] its application in PIC is not reported elsewhere. To the best of our knowledge, this is the first report to use MgO-based PIC in organic conversions.

The Knoevenagel condensation is an important reaction of both academic and industrial relevance. In this reaction, α,β-unsaturated products are formed, which act as useful intermediates in the synthesis of fine chemicals and pharmacological products. Conventionally, this condensation is carried out using various inorganic and organic bases. Many solid bases have been employed as suitable catalysts for this condensation, including MgO.[34,35]

Several strategies have been explored by this research group to accomplish the Knoevenagel condensation through a benign route.[36−39] A new strategy for the Knoevenagel condensation using magnesium oxide (MgO)-stabilized Pickering emulsion as PIC has been developed in the present study. MgO was prepared by precipitation and calcined at different temperatures.

The calcined MgO samples were characterized by the XRD, SEM, TEM, AFM, BET, DLS, and contact angle measurement techniques. The emulsion-stabilizing ability of MgO was studied with respect to the method of preparation, calcination temperature, and solvents.

RESULTS AND DISCUSSION

Characterization of Magnesium Oxide. *XRD.* The XRD pattern of MgO prepared using sodium hydroxide (MgO_S) for precipitation is shown in Figure 1. It has been observed that, at 200 °C, the peaks obtained for 2θ values of 17.92, 32.26, 37.39, 50.22, 58.09, 61.52, 67.69, and 71.33° corresponding to the (011), (100), (101), (102), (110), (111), (103), and (201) planes of $Mg(OH)_2$ match with JCPDS no. 01-075-1527. This indicates an incomplete conversion of $Mg(OH)_2$ to MgO at 200 °C. The diffraction peaks of 36, 42, 62, 74, and 78° obtained for samples calcined at 400, 600, and 800 °C correspond to reflections from the (111), (200), (220), (311), and (222) planes in comparison to JCPDS no. 01-089-7746.

XRD patterns of MgO prepared using ammonium hydroxide (MgO_A) and calcined at the same temperatures as that of MgO_S are similar (Figure 2).

The crystallite size of the calcined samples was calculated by the Debye Scherer formula (eq 1)

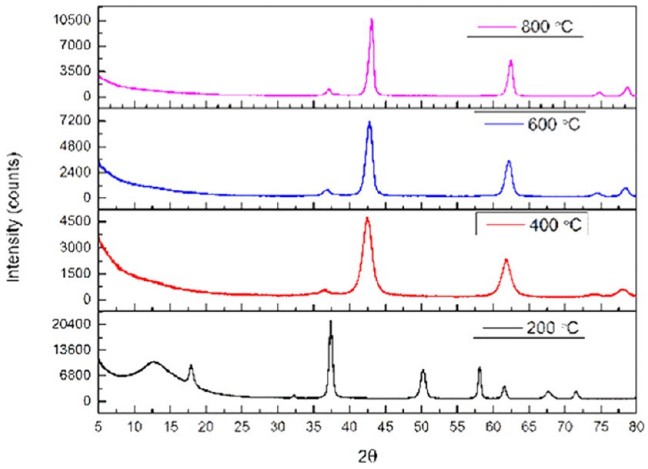

Figure 1. XRD patterns of magnesium oxide prepared using sodium hydroxide (MgO_S).

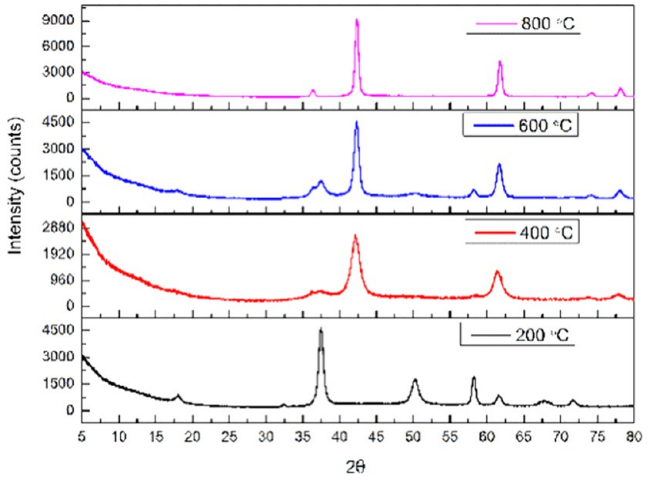

Figure 2. XRD patterns of magnesium oxide prepared using ammonium hydroxide (MgO_A).

Table 1. Crystallite Size of MgO Samples

entry no.	material	crystallite size (nm)
1	MgO_{S_400}	06.65
2	MgO_{S_600}	11.04
3	MgO_{S_800}	15.25
4	MgO_{A_400}	06.04
5	MgO_{A_600}	08.52
6	MgO_{A_800}	12.83

Table 2. BET Surface Area of MgO Samples

entry	sample	BET surface area (m^2/g)
1	MgO_{S_400}	116.67
2	MgO_{S_600}	78.58
3	MgO_{S_800}	58.92
4	MgO_{A_400}	53.53
5	MgO_{A_600}	43.93
6	MgO_{A_800}	35.09

$$\mathrm{Xd} = k\lambda/\beta \cos\theta \quad (1)$$

where Xd is the average crystallite size, k is a dimensionless shape factor ≈0.94, λ is the X-ray wavelength, β is the line broadening at the half-maximum intensity, i.e., full width at

https://dx.doi.org/10.1021/acsomega.0c00819
ACS Omega 2020, 5, 12224−12235

Table 3. Polydispersity Index and Hydrodynamic Diameter of MgO Samples

entry	material	hydrodynamic diameter (nm)	PDI	ζ-potential (mV)
1	MgO_{S_400}	318.4	0.163	+15.9
2	MgO_{S_600}	399.3	0.173	+10.0
3	MgO_{S_800}	300.0	0.225	+10.0
4	MgO_{A_400}	2985	0.138	+7.2
5	MgO_{A_600}	2146	0.265	+6.2
6	MgO_{A_800}	1393	0.322	+7.5

half-maximum height (FWHM) of the most intense peak, and θ is the glancing angle of X-ray with the sample holder.

The crystallite sizes obtained (Table 1) increase from 6.65 to 15.25 nm with an increase in the calcination temperature. The increase in the sharpness of the XRD peaks with respect to the calcination temperature (Figures 1 and 2) also divulges the increase of crystallite size. The method of preparation does not change the crystallite size significantly for a calcination temperature 400 °C but beyond this temperature, it was observed that $MgO_S > MgO_A$.

BET Surface Area. Table 2 shows that MgO_S samples have higher areas than MgO_A. The highest surface area 116.67 m^2/g is obtained for MgO_{A_400}, and it further decreases up to 58.92 m^2/g for MgO_{S_800} (Table 2).

Particle Size, Polydispersity Index, and Zeta Potential (ζ). All of the samples were dispersed in deionized water and sonicated for 5 min before measurement. The hydrodynamic diameter, polydispersity index (PDI), and zeta potentials (ζ) are given in Table 3.

The polydispersity index is a measure of the heterogeneity of dispersed particles. The lower the value of the index, better would be the uniformity in dispersion. The PDI value obtained for all samples is >0.4, which shows that particles are solely dispersed in water.[40] The hydrodynamic diameters of MgO_A (ca. 1300−2900 nm) obtained are 5 times more than those of MgO_S (ca. 300−400 nm). This elucidates from the ζ-potentials of MgO_A being lower, and hence, the electrostatic attraction among the particles is more, due to which particles get agglomerated.

FEG-SEM. The SEM micrographs of MgO prepared by both bases are shown in Figure 3.

The particles obtained by both methods get agglomerated due to strong van der Waals forces between the particles.[41] MgO_S uniformly agglomerates into spherical particles, while the agglomeration is nonuniform in the case of MgO_A. The exact morphology of the particles was confirmed by TEM.

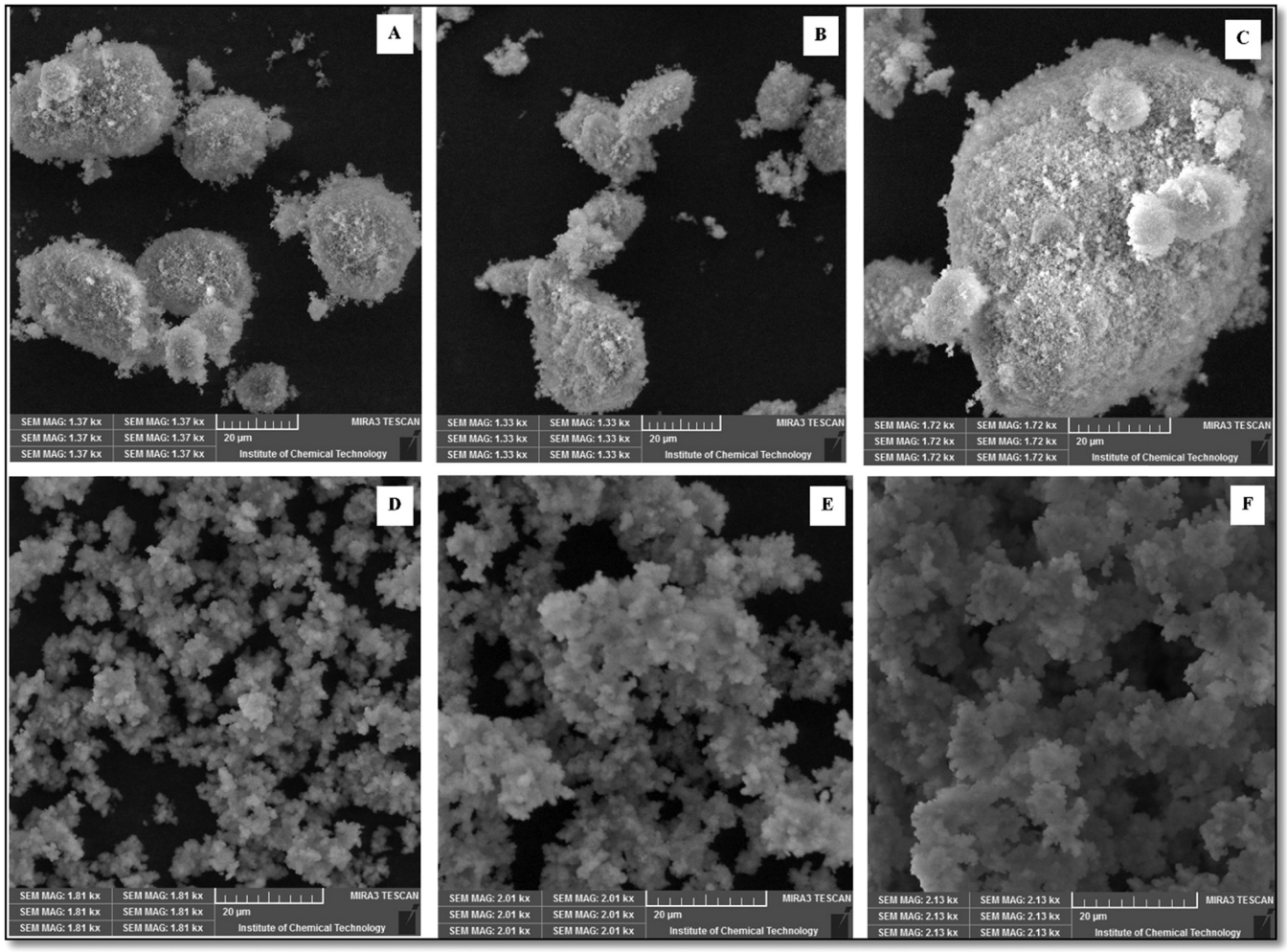

Figure 3. SEM images of magnesium oxide particles: (A) MgO_{S_400}, (B) MgO_{S_600}, (C) MgO_{S_800}, (D) MgO_{A_400}, (E) MgO_{A_600}, and (F) MgO_{A_800}.

https://dx.doi.org/10.1021/acsomega.0c00819
ACS Omega 2020, 5, 12224−12235

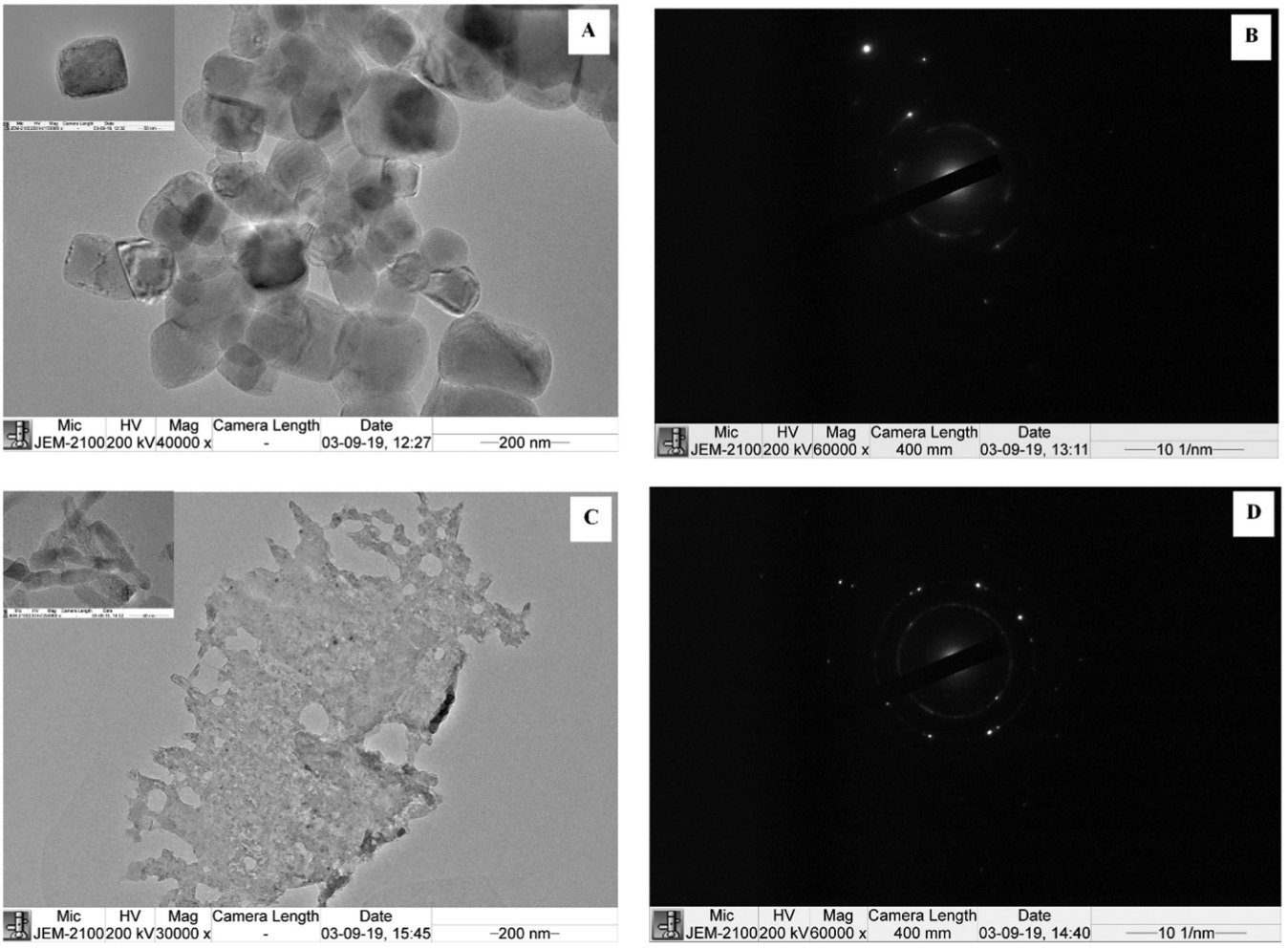

Figure 4. TEM micrographs and the corresponding SAED patterns of (A, B) MgO_{S_400} and (C, D) MgO_{A_400}.

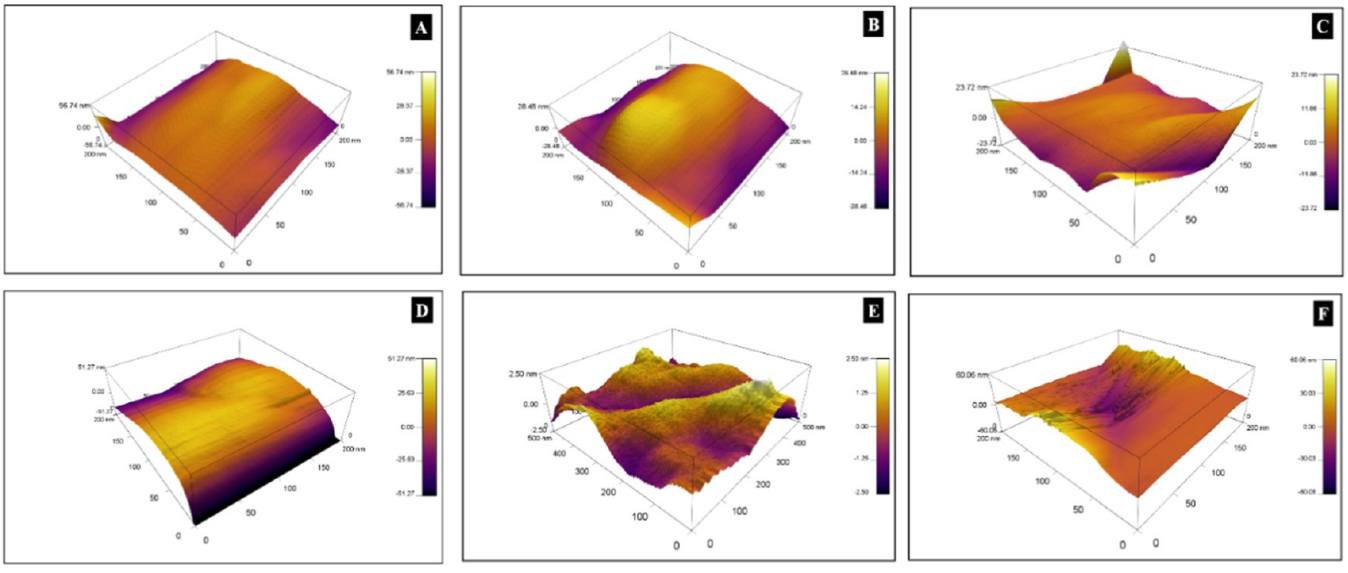

Figure 5. AFM images of (A) MgO_{S_400}, (B) MgO_{S_600}, (C) MgO_{S_800}, (D) MgO_{A_400}, (E) MgO_{A_600}, and (F) MgO_{A_800}.

TEM. Figure 4 depicts the morphology of MgO_S and MgO_A. Particles of partial cubic shape (80−150 nm) were obtained when NaOH was used for precipitation. When a weak base like NH_4OH was used for precipitation, no fixed geometry but elongated rodlike particles were formed. The presence of bright spots in the SAED (selected area electron diffraction) pattern confirms that MgO particles are crystalline (Figure 4B,D). The brightness of spots obtained in MgO_A indicates that the particles are more crystalline. The microscopic surface texture of the MgO particles was further confirmed by AFM.

https://dx.doi.org/10.1021/acsomega.0c00819
ACS Omega 2020, 5, 12224−12235

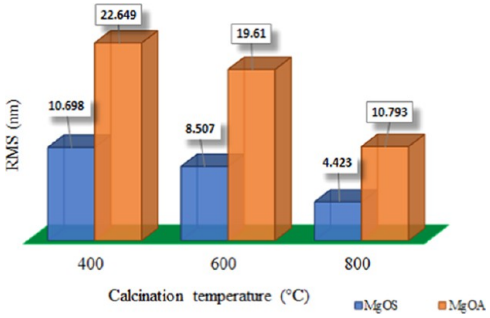

Figure 6. RMS values of magnesium oxide particles.

AFM. The effect of the precipitating agent and calcination temperature on the surface topography of MgO particles is determined by atomic force microscopy (AFM). Figure 5 shows the AFM images of MgO at 200 nm magnification. The surface of MgO_S is smoother than MgO_A at all calcination temperatures.

The root-mean-square (RMS) amplitude (Figure 6) gives a comparison between the particles

The RMS values of MgO_A are higher than those of MgO_S, indicating a rougher surface for the latter sample. It has also been observed that the roughness decreases with an increase in calcination temperature irrespective of the precipitating agent.

The applicability of these surfaces in stabilizing a Pickering emulsion is further predicted by contact angle measurements.

Contact Angle. The presence of metal cations, oxygen anions, and hydroxyl groups on the surfaces of metal oxides makes them hydrophilic.[42] The water contact angles of all prepared MgO samples are less than 90° (Table 4), confirming that MgO is hydrophilic. In the case of MgO_S, the contact angles are around 55°.

The surface roughness affects the contact angle due to the presence of pores and hollows on the surface. The AFM RMS values indicate that the MgO_A surface is rougher and hence the contact angles are lower. In the cases of MgO_{A_400} and MgO_{A_600}, the contact angle could not be determined. In these cases, the liquid directly penetrated the sample, forming contact with a certain angle (entries 4 and 5). An increase in the calcination temperature decreases the roughness, which in turn increases the contact angles, suggesting that the roughness decreases with an increase in the calcination temperature.

Considering all of these aspects, the formation and stability of Pickering emulsion are then studied for MgO particles.

Formation and Stability of Pickering Emulsion. Similar to other metal oxides, magnesium oxide particles are also well known to form stable Pickering emulsion. However, the surface properties affecting the stability of Pickering emulsion in the case of MgO are not taken into account in these reports.

Type of Emulsion. The emulsion type was determined by a drop test, in which the emulsion is simultaneously poured into water and oil in two different Petri dishes. The emulsion type was determined to be O/W. Typically, hydrophilic particles with contact angle <90° will stabilize O/W emulsions and hydrophobic particles with contact angle >90° will stabilize W/O emulsions. The contact angles obtained with MgO samples confirm the emulsion to be of O/W type.[43]

Effect of Surface Properties. Properties such as surface area, surface charge, and surface roughness can be tuned by the proper choice of experimental conditions.

The photographs of emulsions formed using MgO samples as stabilizing agents are shown in Figure 7.

MgO_S stabilizes the emulsion for a longer period (>30 days). The emulsion formed by MgO_A breaks almost immediately, except in the case of MgO_{A_800}, which stabilizes the emulsion for about 30 days. As seen earlier, the surface of MgO_A is rough compared to that of MgO_S.

A liquid drop that comes in contact with a solid surface adheres to the latter, forming a finite contact area only if the total free energy of the system decreases. The contact angle depends on the optimization of the area of contact of the solid/liquid and liquid/vapor interfaces. Contrary to an ideal surface, the real surface can be chemically heterogeneous and/or have surface roughness.

It is interesting to note that the microstructure of the surface can modify the wetting property of the solid surface, which has so far been considered as a macroscopic thermodynamic outcome.

Hence, more refined models of surface contact have been hence developed. The effects of surface heterogeneity and roughness have been considered independently by Cassie and Baxter[44,45] and Wenzel.[46]

Wenzel introduced an "average" contact angle on a rough but chemically homogeneous substrate and expressed the same in terms of the contact angle on a planar one. According to Wenzel, the surface roughness can be related to an apparent contact angle θ^* and the equilibrium contact angle proposed by Young for a smooth surface $\theta\gamma$ as $\cos\theta^* = r\cos\theta\gamma$, where r is the surface roughness.

Table 4. Contact Angles of MgO in Water

Entry	Material	Contact angle (θ)°
1	MgO_{S_400}	52
2	MgO_{S_600}	53
3	MgO_{S_800}	55
4	MgO_{A_400}	–
5	MgO_{A_600}	–
6	MgO_{A_800}	36

https://dx.doi.org/10.1021/acsomega.0c00819
ACS Omega 2020, 5, 12224−12235

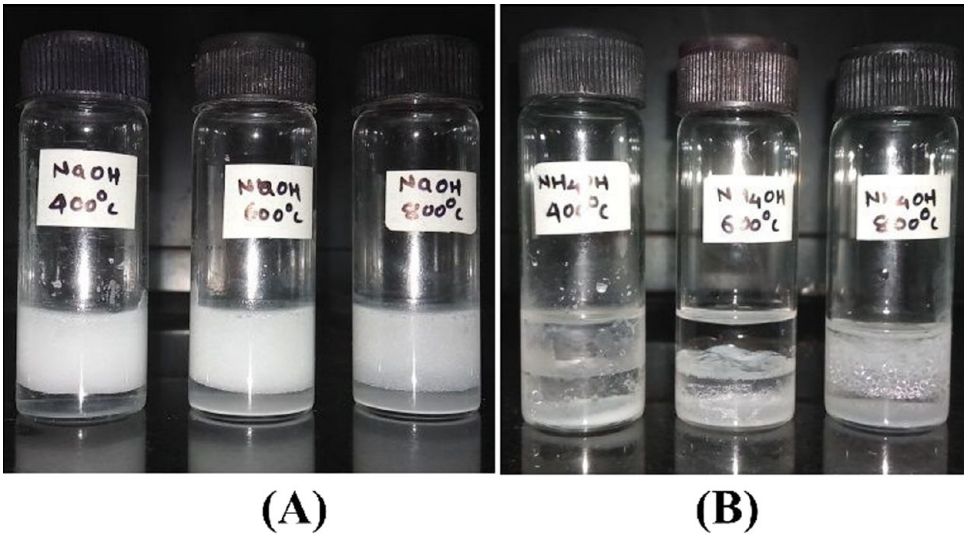

Figure 7. MgO Pickering emulsions: (A) MgO_S and (B) MgO_A (water/toluene = 3:3 mL) (MgO, 20 mg).

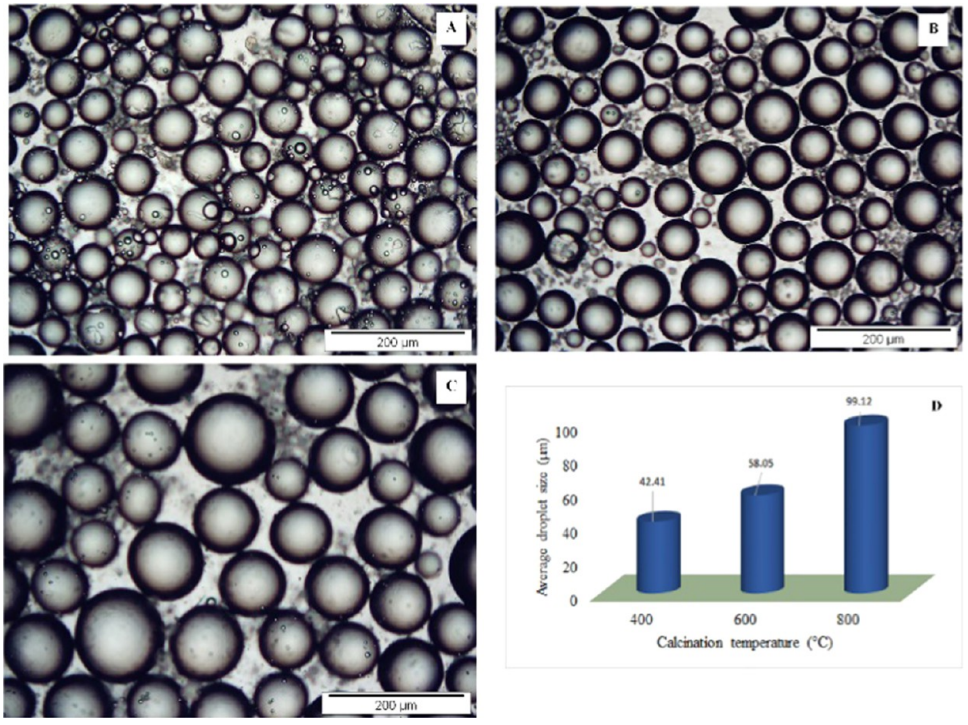

Figure 8. Optical microscopic images of (A) MgO_{S_400}, (B) MgO_{S_600}, and (C) MgO_{S_800} stabilized emulsions. (D) Comparison of average droplet sizes.

From the Wenzel model, it can be deduced that the surface roughness increases the wettability of an original smooth surface. Due to surface roughness, a hydrophilic surface becomes more hydrophilic and a hydrophobic one, more hydrophobic.

The stability of Pickering emulsion is influenced by many factors, including particle size, shape, and concentration, as well as surface wettability. Through extensive research, it has been observed that the major parameter controlling the interfacial behavior and the emulsion stability of Pickering emulsion is wettability. In the present case, it has been observed that the MgO samples with rough surfaces led to the formation of unstable emulsions (Table 4).

The calcination temperature can change the size and shape of solid particles. As the calcination temperature increases, pore volume and crystallite size increase, thereby decreasing the surface area.[47] From Figure 8, the trend of emulsion droplet size can be deduced as MgO_{S_400} < MgO_{S_600} < MgO_{S_800}. This can be attributed to two factors: (i) the droplet size is inversely proportional to the particles available for full coverage of droplet against coalescence[48] and (ii) larger particles repel each other strongly at the interface and do not adsorb at the interface[49] (Figure 9).

While the RMS values of MgO_{S_400} and MgO_{A_800} are nearly equal (Figure 6), the average droplet sizes significantly differ: −42.41 μm for MgO_{S_400} and 341.12 μm for MgO_{A_800}. This may be due to the ζ-potentials of the MgO samples (Table 3).

https://dx.doi.org/10.1021/acsomega.0c00819
ACS Omega 2020, 5, 12224−12235

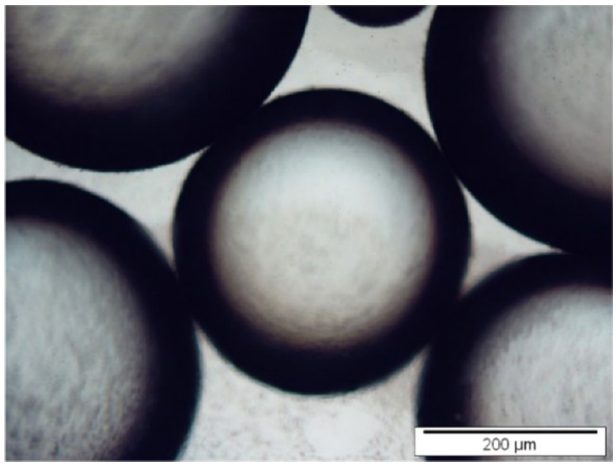

Figure 9. Optical microscopic image of emulsion droplets formed by MgO_{A_800}.

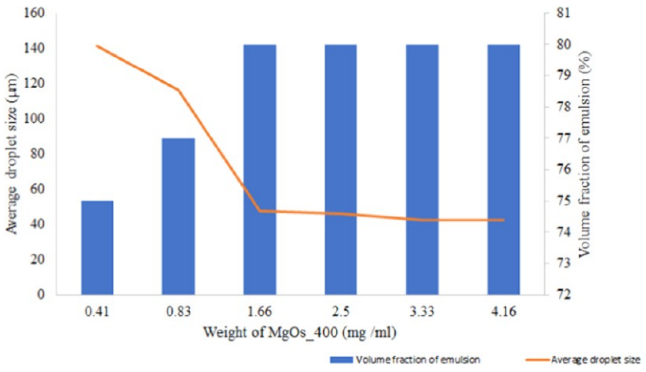

Figure 10. Optimization of the concentration of MgO_{S_400} particles.

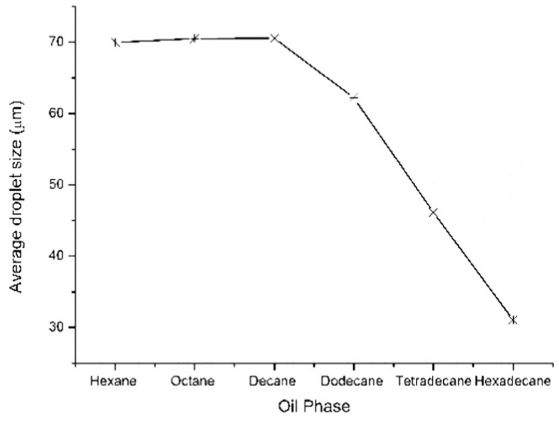

Figure 11. Effect of oil phase on droplets of emulsion.

These values indicate higher attraction among the particles of MgO_{A_800}, which causes their agglomeration, leading to the formation of emulsion with bigger drops.

Effect of MgO Particle Concentration on Pickering Emulsion. A stable emulsion with smaller droplet size is an ideal system for various applications. The optimum particle concentration is a major parameter to form a stable emulsion with smaller droplet size and maximum volume fraction of emulsion.

The results of calcinating the samples at various temperatures reveal that the droplet size of the emulsion formed using MgO_{S_400} is smallest, and hence, this sample was used for further studies. Different quantities (0.41, 0.83, 1.66, 2.50, 3.33, and 4.16 mg/mL mg) of MgO_{S_400} were added to six sample bottles. A constant volume (3 mL) of water was added to each bottle, and the solid was dispersed by ultrasonication. An equal volume of toluene (oil phase) was then added and the bottles were shaken uniformly for about 5 min. The level of creaming was measured by a glass measuring scale, and the droplet size of each emulsion system was determined using a polarizable optical microscope (Figure S1 in the Supporting Information). It has been shown that the effectiveness of colloidal particles to stabilize emulsions largely depends on the formation of a "densely packed" layer of solid particles at the oil−water interface that can sterically inhibit the coalescence of emulsion droplets.[50] An increase in the particle concentration in the emulsion system increases stability either by fully covering the droplet or by forming a new interface, which maximizes the volume fraction of emulsion.

From Figure 10, it can be seen that the volume fraction increases with an increase in MgO_{S_400} concentration (secondary axis). Beyond 1.66 mg/mL MgO particles, about 80% volume fraction of the emulsion stabilized and remained constant at this value. The primary axis reveals that the droplet size decreases with an increase in the amount of MgO_{S_400} and remains constant after 1.66 mg/mL, indicating that sufficient particles are available to cover the droplet.

Effect of Oil Phase. Balanced wetting of the stabilizing solid particles by both the phases leads to the formation of a stable emulsion. If the wetting is preferentially by one of the liquids forming the emulsion, the particles will remain dispersed rather than adsorbed at the interface. The selection of the oil phase is thus an important parameter in forming a stable Pickering emulsion. In this study, various aliphatic hydrocarbons have been tested as oil phase, and the average droplet sizes obtained for the Pickering emulsion stabilized by MgO_{S_400} are shown in Figure 11.

From hexane to hexadecane, there is an increase in surface tension, density, and viscosity. It is observed that these properties associated with the oil phase can affect the adsorption of particles at the interface. The droplet size of emulsion formed with hexane, octane, and decane is approximately the same, while it decreases further with an increase in the chain length. This observation is in good agreement with the trend in surface tension values. As the surface tension of the oil phase increases, the droplet size of the emulsion formed decreases.[51] In the case of hexadecane, the shape of the emulsion droplet changes from spherical to elongated (Figure 12F), indicating that the curvature effect is more dominant for liquids with high viscosity.[52]

The emulsion stability was also tested for some conventionally used organic solvents like toluene, xylene, cyclohexane, dichloromethane, and chloroform. It was observed that the solvents with high density like dichloromethane and chloroform could not form stable emulsion under the conditions employed, while in the cases of toluene, xylene, and cyclohexane, the emulsions were stable under similar conditions.

Application of MgO-Stabilized Pickering Emulsion in Pickering Interfacial Catalysis. The catalytic application of emulsion stabilized by solid MgO particles was studied for the base-catalyzed Knoevenagel condensation reaction. For the reaction between benzaldehyde (4 mmol) and malononitrile (6 mmol), 20 mg of MgO_{S_400} was used as a model reaction (Scheme 1).

https://dx.doi.org/10.1021/acsomega.0c00819
ACS Omega 2020, 5, 12224−12235

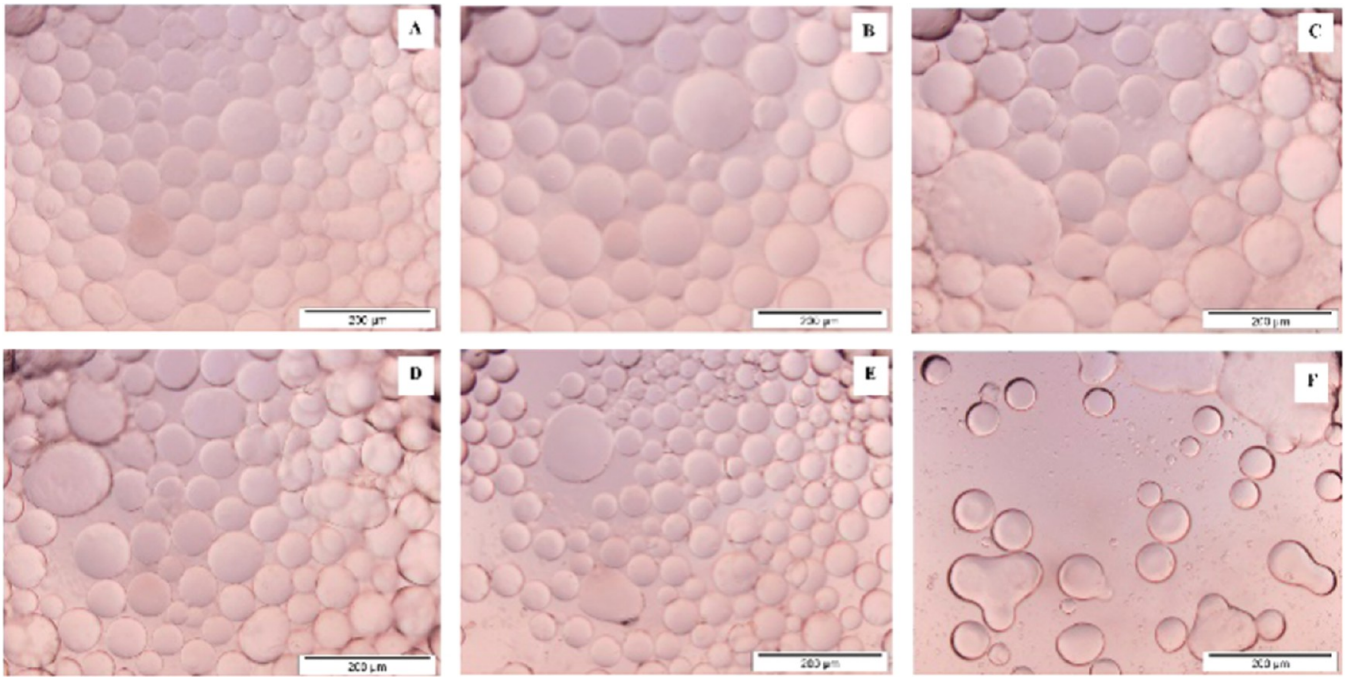

Figure 12. Optical microscopic images of emulsion droplets formed by MgO_{S_400} in different oil phases: (A) hexane, (B) octane, (C) decane, (D) dodecane, (E) tetradecane, and (F) hexadecane.

Scheme 1. Knoevenagel Condensation Reaction

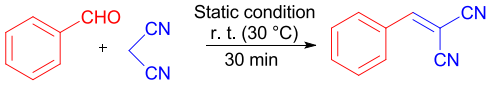

Table 5. Isolated Yield of Condensation Product Using MgO Calcined at Different Temperatures[a]

entry	MgO particles	isolated yield (%)
1	MgO_{S_400}	87
2	MgO_{S_600}	76
3	MgO_{S_800}	67
4	MgO_{A_800}	10

[a]Reaction conditions: benzaldehyde, 4 mmol; malononitrile, 6 mmol; MgO, 20 mg; oil phase, 3 mL; water, 3 mL; room temperature, 30 min.

In a typical reaction procedure, MgO nanoparticles were taken in water and ultrasonicated. An appropriate amount of malononitrile was then added. Benzaldehyde was separately dissolved in toluene and poured into this aqueous phase.

The biphasic system was then agitated to form a stable emulsion.

For catalytic studies, the emulsion was kept at room temperature (30 °C) at static conditions. The progress of the reaction was monitored by gas chromatography. The emulsion forms decrease the mass transfer resistance, and the reaction occurs at the interface.[53] Mechanistically, magnesium oxide abstracts proton from malononitrile generates carbanion, which further attacks the carbonyl carbon of aromatic aldehyde and leads to the formation of α,β-unsaturated product by producing water as a byproduct.[35] It has been observed that the formation of water as a byproduct does not affect the stability of emulsion.

After completion of the reaction, the phases were separated by adding ethyl acetate. Solid particles and unreacted malononitrile remain in the aqueous phase. Unreacted benzaldehyde and the condensation product present in the ester were separated by column chromatography (2:8; ethyl acetate/Pet ether).

Effect of Droplet Size on the Knoevenagel Condensation. The calcination temperature affects the droplet size and also the overall yield of the reaction (Table 5). In each reaction set, 4 mmol of benzaldehyde, 6 mmol of malononitrile, 20 mg of MgO, 3 mL of toluene, and 3 mL of water were used.

It can be seen that MgO_{S_400} that gives emulsions of smaller droplets, thereby generating a larger interfacial area, leads to high yields of the reaction product. Figure 13 represents the PIC system of MgO samples prepared in this study.

Solvent Study for the Knoevenagel Condensation Reaction in MgO-Stabilized Pickering Emulsion. Generally, the polarity of solvent affects the overall yield of the condensation product in the Knoevenagel condensation. As discussed in the above section, only MgO_{S_400} particles are used for forming emulsion and the nonpolar solvents only stabilize the emulsion. The average droplet size of emulsion does not vary by varying the oil phase. Hence, the isolated yield of the product also does not change significantly by changing the solvent (Table 6).

Effect of Substituents. Optimized PIC for the Knoevenagel condensation was extended for the synthesis of substituted α,β-unsaturated products using substituted benzaldehydes (Figure 14). The substitution at benzaldehyde does not affect the formation and stability of the emulsion, and hence, comparable isolated yields are obtained for each substrate. Representative photographs of the reaction systems of substituted benzaldehyde, and the GC-MS, ^{1}H NMR, and ^{13}C NMR spectra of the compounds are given in the Supporting Information (Figures S2−S22).

Reusability of Magnesium Oxide for PIC. After completion of the reaction, the suspended MgO particles were separated from the aqueous phase by centrifugation. The particles were

https://dx.doi.org/10.1021/acsomega.0c00819
ACS Omega 2020, 5, 12224−12235

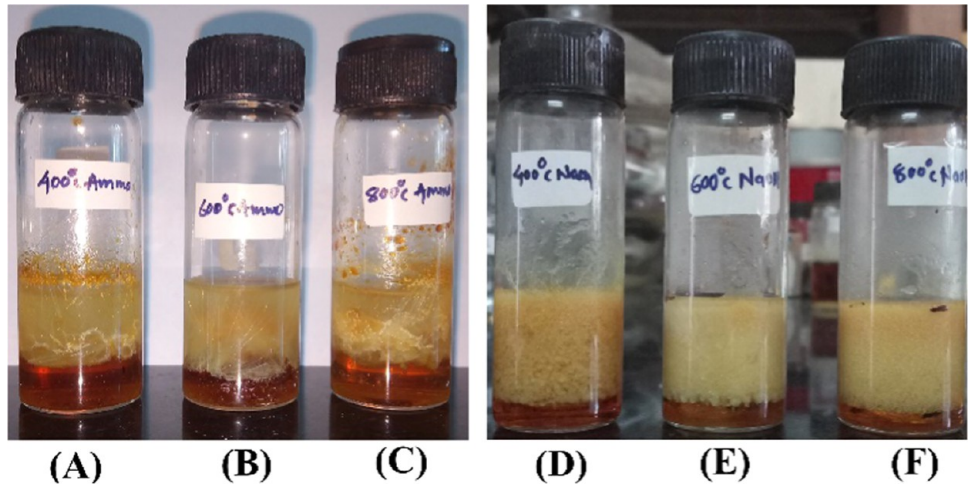

Figure 13. Representative photographs of reaction systems: (A) MgO_{A_400}, (B) MgO_{A_600}, (C) MgO_{A_800}, (D) MgO_{S_400}, (E) MgO_{S_600}, and (F) MgO_{S_800}.

Table 6. Effect of Solvents[a]

entry	solvent	isolated yield (%)
1	hexane	87
2	cyclohexane	80
3	xylene	84
4	toluene	87

[a]Reaction conditions: benzaldehyde, 4 mmol; malononitrile, 6 mmol; MgO_{S_400}, 20 mg; oil phase, 3 mL; water, 3 mL; room temperature, 30 min.

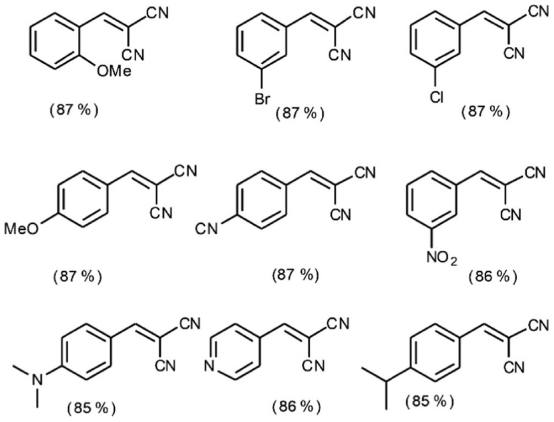

Figure 14. Isolated yield of various substituted α,β-unsaturated condensation products.

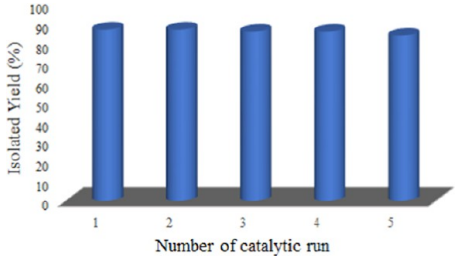

Figure 15. Catalyst reusability in the Knoevenagel condensation.

washed several times with ethanol to remove the adhered organic impurities and dried in a hot-air oven at 100 °C. It was found that a very small amount of MgO (~0.033 mg/mL) was lost during each cycle. It was observed that even after five cycles, the isolated yield does not change significantly (Figure 15).

CONCLUSIONS

A novel green catalytic protocol for the Knoevenagel condensation reaction using magnesium oxide as both base catalyst and emulsion stabilizer has been developed.

Phase-pure MgO obtained by precipitation using a strong base (NaOH) was found to have a smooth surface and could disperse well in water-based emulsions to produce small-droplet-size emulsions compared to the oxide prepared by precipitation using the weak-base (NH_4OH) surface morphology of MgO, and the emulsion stability has been found to have a considerable effect on the catalytic activity.

About 85% yield obtained are for the condensation reactions carried out using MgO_{S_400}, as this material results in the formation of an emulsion with high stability and small emulsion droplet size. However, with MgO_{S_600} and MgO_{S_800}, 76 and 67% yields were obtained under similar reaction conditions. In the cases of MgO_{A_400} and MgO_{A_600}, emulsions were not formed and a very low yield (about 10%) was obtained with MgO_{A_800}. The magnesium oxide suspended in the aqueous phase was separated by centrifugation and recycled for the next run. The use of water as a solvent, reaction at static condition, and the emulsifier itself acting as a solid-base catalyst are the green chemistry advantages of this developed catalytic protocol for the Knoevenagel condensation reaction studied.

MATERIALS AND METHODS

Materials. Magnesium nitrate hexahydrate, sodium hydroxide, ammonium hydroxide solution (25% v/v), ethanol, toluene, xylene, cyclohexane, chloroform, dichloromethane, ethyl acetate, hexane, octane, decane, dodecane, tetradecane, hexadecane, and all substituted aldehydes were purchased from S D Fine-Chem Limited. The chemicals procured were of analytical grade and used without any purification.

Methods. *Preparation of Magnesium Oxide.* Magnesium nitrate hexahydrate ($Mg(NO_3)_2{\cdot}6H_2O$) was dissolved in 100 mL deionized water. An aqueous solution of ammonium hydroxide or sodium hydroxide was added dropwise to this

https://dx.doi.org/10.1021/acsomega.0c00819
ACS Omega 2020, 5, 12224−12235

solution with vigorous stirring at pH 11. After stirring for 2 h at room temperature, the mixture was stored for aging for 24 h. The precipitate obtained was washed with water and ethanol and kept for drying in an air oven at 100 °C for 10 h. The dried samples were calcined at 200, 400, 600, and 800 °C in a muffle furnace for 3 h.[32]

Pickering Emulsion Formation. To prepare the Pickering emulsion, 20.0 mg of MgO was dispersed in water (3 mL) and ultrasonicated to ensure uniform dispersion of particles. The oil phase (3 mL) was then added, and the mixture was emulsified by mechanical agitation. The average drop size of the emulsion was determined using a polarizable optical microscope.

Characterization. *X-ray Diffraction (XRD).* An XRD Bruker D8 ADVANCE instrument was used to analyze the prepared materials. Diffraction intensities were recorded from 5 to 80° using Cu Kα radiation (λ = 1.54 Å).

Field Emission Gun-Scanning Electron Microscopy (FEG-SEM). SEM micrographs of the samples were obtained using a field emission gun-scanning electron microscope (FEG-SEM; Tescan MIRA 3 instrument) with the secondary electron (SE) detector placed between 10.0 and 20.0 kV accelerating voltage.

Transmission Electron Microscopy (TEM). HRTEM analysis was conducted using a TEM JEOL 2010 microscope operating at 200 kV. The samples for HRTEM studies were prepared by depositing a drop of ethanol suspension of the solid sample on a carbon-coated copper grid.

Atomic Force Microscopy (AFM). AFM images were carried out on an Asylum Research Oxford (model no. MFP-3D) AC contact mode instrument using AC-160TS probe at 300 kHz with spring constant K = 26 N/m.

The samples were diluted in methanol and sonicated for 2 min, and the dispersion was poured on a freshly cleaved mica substrate of surface area 4 cm^2. The samples were stored at room temperature to evaporate methanol. All samples were attached to a standard sample puck using double-sided tape.

BET Surface Area Measurements. The surface area of the calcined samples was determined by N_2 sorption at 77 K. Before N_2 sorption, the materials were preheated at 200 °C for 2.5 h by flushing nitrogen to remove the adsorbed gases onto the surface.

Polydispersity Index, Particle Size, and ζ-Potential Measurements. A Malvern Zetasizer (ZS-90, U.K.) was used for determining PDI and ζ-potential.

Contact Angle Measurements. The water contact angle of the samples was measured using a Rame-Hart Goniometer instrument. The powder sample of MgO was compressed using a pelletizer at a pressure of 100 kg/cm^2. A drop of water was placed on the pellet, and equilibrium contact angles were recorded.

Polarized Optical Microscopy. Optical microscope images of the emulsion were obtained using a Bx41 optical microscope fitted with an olympus camera adapter (U-TV0.5XC-3) system using a 5× objective lens.

The average diameter of the droplets was determined with ImageJ v1.47 by measuring the size of 10 droplets from the digital micrographs.

■ ASSOCIATED CONTENT

Supporting Information

The Supporting Information is available free of charge at https://pubs.acs.org/doi/10.1021/acsomega.0c00819.

Optical microscope images—effect of particle concentration of MgO_{S_400} on droplet size; photographs of the reaction system for substituted benzaldehydes; GC-MS spectra of α,β-unsaturated condensation products; and ^{1}H NMR and ^{13}C NMR of α,β-unsaturated condensation products (PDF)

■ AUTHOR INFORMATION

Corresponding Author

Radha V. Jayaram − *Department of Chemistry, Institute of Chemical Technology, Mumbai 400019, India;* orcid.org/0000-0002-8392-7674; Email: rv.jayaram@ictmumbai.edu.in

Authors

Amid L. Sadgar − *Department of Chemistry, Institute of Chemical Technology, Mumbai 400019, India*

Tushar S. Deore − *Department of Chemistry, Institute of Chemical Technology, Mumbai 400019, India*

Complete contact information is available at: https://pubs.acs.org/10.1021/acsomega.0c00819

Notes

The authors declare no competing financial interest.

■ ACKNOWLEDGMENTS

A.L.S. is thankful to Department of Atomic Energy (DAE) for the junior research fellowship, and T.S.D. is thankful to University Grants Commission (UGC) for senior research fellowship. The authors also acknowledge Department of Bioscience and Bioengineering, Indian Institute of Technology Bombay (IITB), for providing AFM facility.

■ REFERENCES

(1) La Sorella, G.; Strukul, G.; Scarso, A. Recent advances in catalysis in micellar media. *Green Chem.* **2015**, *17*, 644−683.

(2) Starks, C. M. Phase-transfer catalysis. I. Heterogeneous reaction involving anion transfer by quaternary ammonium and phosphonium salts. *J. Am. Chem. Soc.* **1971**, *93*, 195−199.

(3) Noyori, R.; Aoki, M.; Sato, K. Green oxidation with aqueous hydrogen peroxide. *Chem. Commun.* **2003**, 1977−1986.

(4) Öztürk, B. Ö.; Öztürk, S. Transfer-hydrogenation reactions of ketones/aldehydes in water using first generation ruthenium indenylidene olefin metathesis catalyst: one step towards sequential cross-metathesis/transfer hydrogenation reactions. *Mol. Catal.* **2020**, *480*, No. 110640.

(5) Le Quéméner, F.; Subervie, D.; Morlet-Savary, F.; Lalevée, J.; Lansalot, M.; Bourgeat-Lami, E.; Lacôte, E. Visible-Light Emulsion Photopolymerization of Styrene. *Angew. Chem., Int. Ed.* **2018**, *57*, 957−961.

(6) Lesage, G.; Quesada, I.; Franceschi, S.; Perez, E.; Garrigues, J.-C.; Martine, P.; Patrick, C. Sustainable process for adipic acid production from cyclohexene in microemulsion. *Catal. Today* **2020**, 40−45.

(7) Pogrzeba, T.; Schmidt, M.; Milojevic, N.; Urban, C.; Illner, M.; Repke, J. U.; Schomäcker, R. Understanding the Role of Nonionic Surfactants during Catalysis in Microemulsion Systems on the Example of Rhodium-Catalyzed Hydroformylation. *Ind. Eng. Chem. Res.* **2017**, *56*, 9934−9941.

(8) Petcu, A. R.; Meghea, A.; Rogozea, E. A.; Olteanu, N. L.; Lazar, C. A.; Cadar, D.; Crisciu, A. V.; Mihaly, M. No Catalyst Dye Photodegradation in a Microemulsion Template. *ACS Sustainable Chem. Eng.* **2017**, *5*, 5273−5283.

(9) Manabe, K.; Iimura, S.; Sun, X.-M.; Kobayashi, S. Dehydration Reactions in Water. Brønsted Acid−Surfactant-Combined Catalyst for

Ester, Ether, Thioether, and Dithioacetal Formation in Water. *J. Am. Chem. Soc.* **2002**, *124*, 11971−11978.
(10) Pickering, S. U. CXCVI.—emulsions. *J. Chem. Soc., Trans.* **1907**, *91*, 2001−2021.
(11) Nuumani, R. L.; Vladisavljević, G. T.; Kasprzak, M.; Wolf, B. In-vitro oral digestion of microfluidically produced monodispersed W/O/W food emulsions loaded with concentrated sucrose solution designed to enhance sweetness perception. *J. Food Eng.* **2020**, *267*, No. 109701.
(12) Sy, P. M.; Anton, N.; Idoux-gillet, Y.; Dieng, S. M.; Messaddeq, N.; Ennahar, S.; Diarra, M.; Vandamme, T. F. Pickering nanoemulsion as a nanocarrier for pH-triggered drug release. *Int. J. Pharm.* **2018**, *549*, 299−305.
(13) Shankar, R.; Jangir, B.; Sharma, A. A novel synthetic approach to poly(hydrosiloxane)s via hydrolytic oxidation of primary organosilanes with a AuNPs-stabilized Pickering interfacial catalyst. *RSC Adv.* **2017**, *7*, 344−351.
(14) Lv, G.; Wang, F.; Zhang, X.; Binks, B. P. Surface-Active Hollow Titanosilicate Particles as a Pickering Interfacial Catalyst for Liquid-Phase Alkene Epoxidation Reactions. *Langmuir* **2018**, *34*, 302−310.
(15) Ikeda, S.; Nur, H.; Sawadaishi, T.; Ijiro, K.; Shimomura, M.; Ohtani, B. Direct Observation of Bimodal Amphiphilic Surface Structures of Zeolite Particles for a Novel Liquid-Liquid Phase Boundary Catalysis. *Langmuir* **2001**, *17*, 7976−7979.
(16) Zhang, Y.; Zhang, H.; Liu, P.; Sun, H.; Li, B.-G.; Wang, W.-J. Programming Hydrogen Production via Controllable Emulsification/Demulsification in a Switchable Oil−Water System. *ACS Sustainable Chem. Eng.* **2019**, *7*, 7768−7776.
(17) Tang, J.; Zhou, X.; Cao, S.; Zhu, L.; Xi, L.; Wang, J. Pickering Interfacial Catalysts with CO_2 and Magnetic Dual Response for Fast Recovering in Biphasic Reaction. *ACS Appl. Mater. Interfaces* **2019**, *11*, 16156−16163.
(18) Pera-Titus, M.; Leclercq, L.; Clacens, J.-M.; Campo, F. D.; Nardello-Rataj, V. Pickering Interfacial Catalysis for Biphasic Systems: From Emulsion Design to Green Reactions. *Angew. Chem., Int. Ed.* **2015**, *54*, 2006−2021.
(19) Shan, Y.; Yu, C.; Yang, J.; Dong, Q.; Fan, X.; Qiu, J. Thermodynamically Stable Pickering Emulsion Configured with Carbon-Nanotube-Bridged Nanosheet-Shaped Layered Double Hydroxide for Selective Oxidation of Benzyl Alcohol. *ACS Appl. Mater. Interfaces* **2015**, *7*, 12203−12209.
(20) Tang, J.; Cao, S.; Wang, J. CO_2-switchable Pickering emulsions: efficient and tunable interfacial catalysis for alcohol oxidation in biphasic systems. *Chem. Commun.* **2019**, *55*, 11079−11082.
(21) Yang, H.; Zhou, T.; Zhang, W. A Strategy for Separating and Recycling Solid Catalysts Based on the pH-Triggered Pickering-Emulsion Inversion. *Angew. Chem., Int. Ed.* **2013**, *52*, 7455−7459.
(22) Tao, L.; Zhong, M.; Chen, J.; Jayakumar, S.; Liu, L.; Li, H.; Yang, Q. Heterogeneous hydroformylation of long-chain alkenes in IL-in-Oil Pickering Emulsion. *Green Chem.* **2018**, *20*, 188−196.
(23) Chen, S.; Zhang, F.; Yang, M.; Li, X.; Liang, H.; Qiao, Y.; Liu, D.; Fan, W. A simple strategy towards the preparation of a highly active bifunctionalized catalyst for the deacetalization reaction. *Appl. Catal., A* **2016**, *513*, 47−52.
(24) Xue, F.; Zhang, Y.; Zhang, F.; Ren, X.; Yang, H. Tuning the Interfacial Activity of Mesoporous Silicas for Biphasic Interface Catalysis Reactions. *ACS Appl. Mater. Interfaces* **2017**, *9*, 8403−8412.
(25) Yang, X.; Liang, Y.; Cheng, Y.; Song, W.; Wang, X.; Wang, Z.; Qiu, J. Hydrodeoxygenation of vanillin over carbon nanotube-supported Ru catalysts assembled at the interfaces of emulsion droplets. *Catal. Commun.* **2014**, *47*, 28−31.
(26) Shi, H.; Fan, Z.; Hong, B.; Pera-Titus, M. Aquivion Perfluorosulfonic Superacid as an Efficient Pickering Interfacial Catalyst for the Hydrolysis of Triglycerides. *ChemSusChem* **2017**, *10*, 3363−3367.
(27) Yang, B.; Leclercq, L.; Clacens, J.-M.; Nardello-Rataj, V. Acid/amphiphilic silica nanoparticles: new eco-friendly Pickering interfacial catalysis for biodiesel production. *Green Chem.* **2017**, *19*, 4552−4562.
(28) Tang, J.; Zhang, Q.; Hu, K.; Cao, S.; Zhang, S.; Wang, J. Novel organic base-immobilized magneto-polymeric nanospheres as efficient Pickering interfacial catalyst for transesterification. *J. Catal.* **2018**, *368*, 190−196.
(29) Zhang, S.; Hong, B.; Fan, Z.; Lu, J.; Xu, Y.; Pera-Titus, M. Aquivion-Carbon Composites with Tunable Amphiphilicity for Pickering Interfacial Catalysis. *ACS Appl. Mater. Interfaces* **2018**, *10*, 26795−26804.
(30) Kantam, M. L.; Redddy, P. V.; Srinivas, P.; Venugopal, A.; Bhargava, S.; Nishina, Y. Nanocrystalline magnesium oxide-stabilized palladium(0): the Heck Reaction of heteroaryl bromides in the absence of additional ligands and base. *Catal. Sci. Technol.* **2013**, *3*, 2550−2554.
(31) Sy, P. M.; Dieng, S. M.; Diouf, L. A. D.; Djiboune, A. R.; Soumboundou, M.; Ndong, B.; Diop, O.; Bathily, E. H. A. L.; Mbaye, G.; Diouf, M.; Mbodj, M.; Diarra, M. Tramadol Encapsulation in Aqueous Phase of Water/Oil Pickering Emulsion Stabilized by Magnesium Oxide Particles. *Int. J. Biochem. Biophys.* **2018**, *6*, 37−43.
(32) Elmotasem, H.; Farag, H. K.; Salama, A. A. A. In vitro and in vivo evaluation of an oral sustained release hepatoprotective caffeine Loaded w/o Pickering Emulsion Formula − containing wheat germ oil and stabilized by magnesium oxide nanoparticles. *Int. J. Pharm.* **2018**, *547*, 83−96.
(33) Sy, P. M.; Djiboune, A. R.; Diouf, L. A. D.; Soumboundou, M.; Ndong, B.; Ndiaye, A.; Dieng, S. D.; Diop, O.; Bathily, E. H. A. L.; Mbaye, G.; Faye, M.; Mbodj, M.; Diarra, M. Water/Oil Pickering Emulsion Stabilized by Magnesium Oxide Particles: A Potential System with Two Active Substances (Paracetamol and Griseofulvin). *Open J. Biophys.* **2018**, *8*, 68−84.
(34) Vidruk, R.; Landau, M. V.; Herskowitz, M.; Talianker, M.; Frage, N.; Ezersky, V.; Froumin, N. Grain boundary control in nanocrystalline MgO as a novel means for significantly enhancing surface basicity and catalytic activity. *J. Catal.* **2009**, *263*, 196−204.
(35) Xu, C. L.; Bartley, J. K.; Enache, D. I.; Knight, D. W.; Hutchings, G. H. High Surface Area MgO as a Highly Effective Heterogeneous Base Catalyst for Michael Addition and Knoevenagel Condensation Reactions. *Synthesis* **2005**, *19*, 3468−3476.
(36) Gawande, M. B.; Jayaram, R. V. A novel catalyst for the Knoevenagel condensation of aldehydes with malononitrile and ethyl cyanoacetate under solvent free conditions. *Catal. Commun.* **2006**, *7*, 931−935.
(37) Shrikhande, J. J.; Gawande, M. B.; Jayaram, R. V. Cross-aldol and Knoevenagel condensation reactions in aqueous micellar media. *Catal. Commun.* **2008**, *9*, 1010−1016.
(38) Thakare, S. C.; Jayaram, R. V. Amino-Functionalized Activated Carbon Materials in Base-Catalyzed Reactions. *Catal. Green Chem. Eng.* **2018**, *1*, 113−126.
(39) Sahani, A. J.; Burange, A. S.; Jayaram, R. V. An efficient Knoevenagel condensation of aldehydes with active methylene compounds over novel, robust CeZrO4-δ catalyst. *Res. Chem. Intermed.* **2018**, *44*, 7805−7814.
(40) Mehta, M.; Mukhopadhyay, M.; Christian, R.; Mistry, N. Synthesis and characterization of MgO nanocrystals using strong and weak bases. *Powder Technol.* **2012**, *226*, 213−221.
(41) Jeevanandam, J.; Chan, Y. S.; Danquah, M. K. Biosynthesis and characterization of MgO nanoparticles from plant extracts via induced molecular nucleation. *New J. Chem.* **2017**, *41*, 2800−2814.
(42) Bae, J.; Samek, I. A.; Stair, P. C.; Snurr, R. Q. Investigation of the Hydrophobic Nature of Metal Oxide Surfaces Created by Atomic Layer Deposition. *Langmuir* **2019**, *35*, 5762−5769.
(43) Zhou, J.; Qiao, X.; Binks, B. P.; Sun, K.; Bai, M.; Li, Y.; Liu, Y. Magnetic Pickering Emulsions Stabilized by Fe_3O_4 Nanoparticles. *Langmuir* **2011**, *27*, 3308−3316.
(44) Cassie, A. B. D.; Baxter, S. Wettability of Porous Surfaces. *Trans. Faraday Soc.* **1944**, *40*, 546−551.
(45) Zhang, X.; Zheng, Y.; Feng, X.; Han, X.; Bai, Z.; Zhang, Z. Calcination temperature-dependent surface structure and physicochemical properties of magnesium oxide. *RSC Adv.* **2015**, *5*, 86102−86112.

https://dx.doi.org/10.1021/acsomega.0c00819
ACS Omega 2020, 5, 12224−12235

(46) Wenzel, R. N. Resistance of Solid Surfaces to Wetting by Water. *Ind. Eng. Chem.* **1936**, *28*, 988−994.
(47) Whitby, C. P.; Parthipan, R. Influence of particle concentration on multiple droplet formation in pickering emulsions. *J. Colloid Interface Sci.* **2019**, *554*, 315−323.
(48) Nallamilli, T.; Mani, E.; Basavaraj, M. G. A Model for the Prediction of Droplet Size in Pickering Emulsions Stabilized by Oppositely Charged Particles. *Langmuir* **2014**, *30*, 9336−9345.
(49) Wang, J.; Yu, M.; Yang, C. Colloidal TiO_2 Nanoparticles with near-neutral wettability: An efficient Pickering Emulsifier. *Colloids Surf., A* **2019**, *570*, 224−232.
(50) Tambe, D. E.; Sharma, M. M. The effect of colloidal particles on fluid-fluid interfacial properties and emulsion stability. *Adv. Colloid Interface Sci.* **1994**, *52*, 1−63.
(51) Zhang, Y.; Chen, K.; Cao, L.; Li, K.; Wang, Q.; Fu, E.; Guo, X. Stabilization of Pickering Emulsions by Hairy Nanoparticles Bearing Polyanions. *Polymers* **2019**, *11*, 816.
(52) Dai, L. L.; Tarimala, S.; Wu, C.-W.; Guttula, S.; Wu, J. The Structure and Dynamics of Microparticles at Pickering Emulsion Interfaces. *Scanning* **2008**, *30*, 87−95.
(53) Qian, B.; Wang, F.; Li, D.; Li, Y.; Zhang, B.; Zhu, J. Preparation of Pickering emulsion by modification of amine-functionalized graphene oxide surface with organosilane: Efficient catalyst for Knoevenagel condensation of malononitrile with aldehydes at mild temperature. *New J. Chem.* **2020**, *44*, 5995−6002.

https://dx.doi.org/10.1021/acsomega.0c00819
ACS Omega 2020, 5, 12224−12235